A Broadband U-Slot Coupled Microstrip-to-Waveguide Transition

Xiaobo Huang and Ke-Li Wu, *Fellow, IEEE*

***Abstract*—A novel planar broadband microstrip-to-waveguide transition is proposed in this paper. The referred waveguide can be either rectangular waveguide or ridged waveguide. The transition consists of an open-circuited microstrip quarter-wavelength resonator and a resonant U-shaped slot on the upper broadside wall of a short-circuited waveguide. A physics-based equivalent-circuit model is also developed for interpreting the working mechanism and providing a coarse model for engineering design. The broadband transition can be regarded as a stacked two-pole resonator filter. Each coupling circuit can be approximately designed separately using the group-delay information at the center frequency. In addition to its broadband attribute, the transition is compact in size, vialess, and is highly compatible with planar circuits. These good features make the new transition very attractive for the system architecture where waveguide devices need to be surface mounted on a multilayered planer circuit. Two design examples are given to demonstrate the usefulness of the transition: one is a broadband ridged-waveguide bandpass filter and the other is a surface-mountable broadband low-temperature co-fired ceramic laminated waveguide cavity filter. Both filters are with the proposed transition for interfacing with microstrip lines, showing promising potentials in practical applications.**

***Index Terms*—Broadband, laminated waveguide, microstrip-to-waveguide transition, ridged waveguide, transition, waveguide filters.**

I. Introduction

IN COMMERCIAL and military communication systems operating in microwave and millimeter-wave frequencies, microstrip and waveguide are the two most commonly used transmission lines for effectively transferring high-frequency signals among various modules. Microstrip lines are often used for connecting multiple active circuit modules involving transistors, monolithic microwave integrated circuits (MMICs), and various surface mounted components, whereas waveguides are usually the first choice for antenna feed network, high Q filters, and low-loss transmission lines if space is permitted.

In a system architecture design, it is advantageous to have coexisting modules that use different types of transmission line, such as microstrip lines and waveguides. In this connection, a broadband microstrip-to-waveguide transition is required when a waveguide device needs to be connected with a module whose interfacing transmission line is microstrip. In many applications, such inter-connections are preferred to be surface mounted on a multilayered system board. Therefore, developing a broadband microstrip-to-waveguide transition, which is conformal to a planar substrate, easy to fabricate, and more importantly compact in size, is a very important subject. In addition to meeting the increasing demands on signal bandwidth, a broadband transition also provides other attractive characteristics, such as low insertion loss and less manufacturing tolerance requirement.

There are many microstrip-to-waveguide transition configurations proposed in the past. The earliest published work can be traced back to 1967 [1]. The existing microstrip-to-waveguide transitions can be classified into three categories: the probe insert type, impedance-taper type, and aperture coupled type. For the probe insert type, the probe can be considered as a kind of extension of the microstrip line that is inserted into the waveguide from either a sidewall or the end wall. Various probe configurations were proposed for broadening the working bandwidth. Some prior works in this category include patch probe [2], Yagi antenna-like probe [3], gradually tapered ridges at opposite sides of an inserted dielectric substrate and a T-shaped probe with an impedance transformer [4], [5], and radial-shaped probe [6]. The probe-type transitions are usually not conformal to planar circuits. The most unfavorable feature of these types of transitions is the inconvenience of installation for mass production, particularly in millimeter-wave applications due to their nonplanar structure in nature. The impedance taper type of transitions can be considered as an improvement of the probe insert type in terms of conformity to planar circuits. The popular approaches in this category use multisection ridged-waveguide impedance stairs or microstrip taper to convert the quasi-TEM mode of microstrip line to a TE_{10} dominant mode in rectangular waveguide [7]–[9]. Although the structure allows a waveguide device to be integrated with other planar circuits, its oversized dimensions and the narrow bandwidth would be the limitations for many applications. On the other hand, aperture coupled transitions were also investigated by many researchers in the past. It is interesting that in all these aperture coupled microstrip-to-waveguide transitions found in the literature, the signal is coupled at the end wall or narrow sidewall of the waveguide [10]–[13] and the apertures are small in terms of wavelength. It is understandable that the electric field coupled by an electrically small aperture at the end wall of rectangular waveguide is in line with the TE_{10} mode, and with an appropriate matching element the mode

Manuscript received June 27, 2011; revised January 03, 2012; accepted January 05, 2012. Date of publication March 08, 2012; date of current version April 27, 2012. This work was supported in part by the Research Grants Council of the Hong Kong Special Administrative Region under Grant 2150499.

X. Huang was with the Department of Electronic Engineering, The Chinese University of Hong Kong, Shatin, Hong Kong. He is now with the China Research and Development Center, Comba Telecommunication Systems, Guangzhou 510530, China (e-mail: xbhuang@ee.cuhk.edu.hk).

K.-L. Wu is with the Department of Electronic Engineering, The Chinese University of Hong Kong, Shatin, Hong Kong (e-mail: klwu@ee.cuhk.edu.hk).

Color versions of one or more of the figures in this paper are available online at http://ieeexplore.ieee.org.

Digital Object Identifier 10.1109/TMTT.2012.2187677

can be excited effectively. Nevertheless, considering the conformity to planar circuits and the convenience of installation for high-volume production, the broadside wall aperture coupled microstrip-to-waveguide transitions would be a favorite configuration for system integrations. Therefore, developing a new coupling mechanism with a slot on the broadside wall of a waveguide and an effective circuit structure for transferring the broadband signal is an important subject.

In this paper, a novel broadband microstrip-to-waveguide transition is proposed. The transition is analogous to a two-pole resonator filter with two resonant poles (reflection zeros) in the passband. For clearly revealing the working principle and providing an engineering design guideline, a physics-based equivalent-circuit model for the transition is also developed. Based on the equivalent-circuit model, the coupling coefficients of the physical circuit model can be expressed in terms of group-delay information of an approximated individual sub-circuit model. For a typical application in microwave frequencies, more than 55% bandwidth for the return loss better than 15 dB can be achieved. In addition to the excellent broadband performance, the new vialess transition will be an attractive choice for system integration in terms of its compact size, the conformity to planar circuits, and the simplicity in manufacturing for mass production.

The declared features are demonstrated through two filter design examples: one is a surface mountable broadband ridged-waveguide filter; the other is a surface mountable low-temperature co-fired ceramic (LTCC) laminated waveguide filter module. Both are in C-band. To show the broadband feature of a standalone transition, a back-to-back microstrip-waveguide-microstrip test module was designed, manufactured, and tested. The two filter examples were designed by following the given design formula and full-wave electromagnetic (EM) simulation tool Ansoft HFSS. The designed modules were manufactured and verified by experiment. Very good agreement between the measured and simulated results is shown, which further verifies the proposed transition structure and the design procedure.

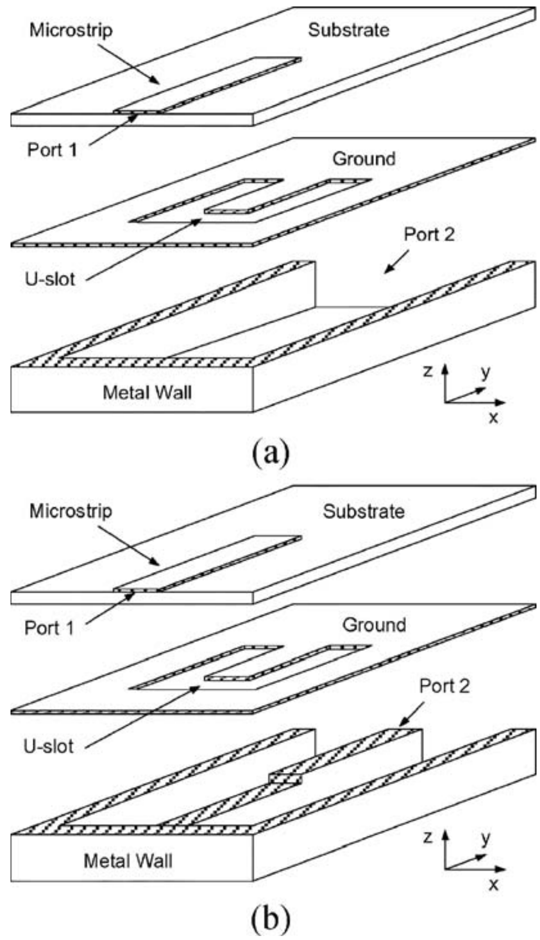

Fig. 1. Structure of the proposed transition. (a) Microstrip-to-rectangular waveguide transition. (b) Microstrip-to-ridged-waveguide transition.

II. Configuration of the Transition

The proposed transition consists of an open-circuited quarter-wavelength microstrip line resonator that is directly coupled to the input microstrip line, a half-wavelength resonant U-shaped slot on the substrate ground plane, which also serves as a broadside wall of the waveguide, and a short-circuited waveguide underneath the ground plane. The waveguide here is defined as a single conductor tube with the electric field of its dominant mode perpendicular to the broadside wall. Both rectangular waveguide and ridged waveguide fall into the category. Fig. 1(a) and (b) shows an exploded view of the proposed transition for a microstrip line to rectangular waveguide transition and a microstrip line to ridged-waveguide transition, respectively.

In the transition structure, the microstrip line printed on a dielectric substrate is placed perpendicularly to the short middle section of the U-shaped slot. The coupling between them can be controlled by the width of the slotline and an offset displacement from the center. In general, the characteristic impedance of the input microstrip line and that of the open-circuited quarter-wavelength transmission line can be different for controlling the coupling between them. The open end is deliberately placed approximately $\lambda_g/4$ away from the middle section for creating an open-circuited resonator. Being a U-shaped half wavelength slotline resonator, the transition only occupies a space of less than a quarter-wavelength.

The waveguide is short circuited at the end near the middle section of the U-shaped slot and the other end defines as a port of the transition. The coupling between the waveguide and the half-wavelength U-shaped slotline resonator can be controlled by introducing an obstacle in the waveguide section that is in the vicinity of the slotline resonator. Such an obstacle can be a tuning screw or an impedance step, as illustrated in the transition for ridged waveguide shown in Fig. 1(b).

The working mechanism of the proposed transition can be explained by the concept of a two-pole resonator filter having two resonant poles in the passband. As compared to the conventional transitions of prior art, the proposed transition provides a much wider bandwidth, and consequently, lower insertion loss.

III. Physics-Based Equivalent-Circuit Model

In order to reveal the working mechanism of the transition, an equivalent-circuit model using transmission lines and ideal transformers is given in Fig. 2. The circuit model comprises three transformers, an open-circuited quarter-wavelength

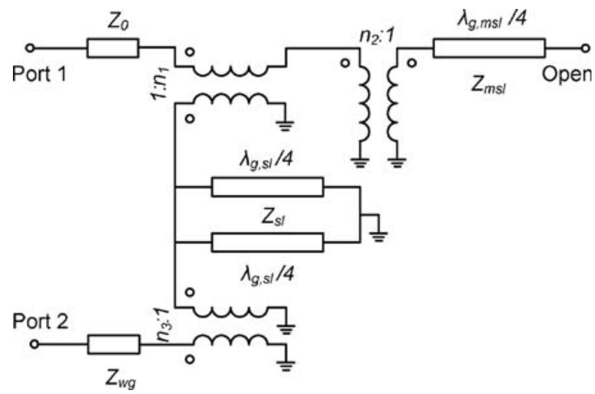

Fig. 2. Equivalent-circuit model of the proposed microstrip-to-waveguide transition.

resonator and two shunt short-circuited quarter-wavelength resonators. The transformers in the circuit represent the EM couplings between the input/output transmission lines and the resonators. The U-shaped slot is represented by two parallel short-circuited quarter-wavelength slotline resonators and acts as a middleman between the two types of transmission line. Specifically, transformer n_1 represents the coupling between the U-shaped slotline resonator and the microstrip line. Transformer n_2 describes the coupling between the open-circuited quarter-wavelength resonator and the microstrip line. Similar to transformer n_1, n_3 depicts the coupling between the slotline resonator and the waveguide.

A. Coupling for Open-Circuited Resonator

In the equivalent-circuit model shown in Fig. 2, there are two interlaced resonators: an open-circuited quarter-wavelength microstrip resonator and a pair of shunt short-circuited slotline quarter-wavelength resonators. Having appropriately determined the dimensions of the two resonators for a giving center frequency, designing the physical dimensions for realizing the three coupling transformers, namely, n_1, n_2, and n_3, will be critical.

It is known that an open-circuited quarter-wavelength resonator can be approximated by a series LC resonant circuit. Therefore, the coupling circuit of the input microstrip line and the quarter-wavelength open-circuited resonator as depicted in Fig. 3(a) can be represented by the lumped-element circuit of Fig. 3(b). Note that by definition of an ideal transformer with turns ratio n, there is $R' = R/n^2$, where R' is the resistance looking toward the transformer from the resonator and R is the source resistance, or the characteristic impedance Z_0 of the input microstrip line in the physical model. Therefore, the external Q of the LC series resonant circuit of Fig. 3(b) at the resonant frequency $\omega_0 = 1/\sqrt{LC}$ is

$$Q_e = \frac{\omega_0 L}{R'} = \sqrt{\frac{L}{C}} \cdot \frac{1}{R'} = {n_2}^2 \sqrt{\frac{L}{C}} \cdot \frac{1}{R}. \tag{1}$$

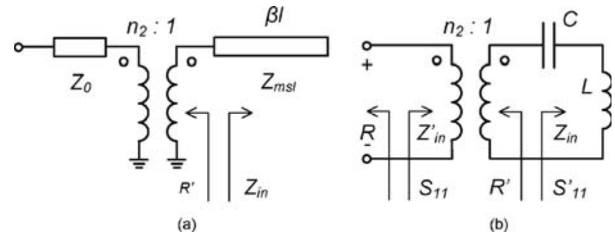

Fig. 3. (a) Coupling circuit between a transmission line and an open-circuited $\lambda/4$ resonator by an ideal transformer. (b) Corresponding lumped-element circuit model.

For the quarter-wavelength open-circuited resonant circuit in Fig. 3(a), where $l = \lambda/4$, in the vicinity of resonant frequency $\omega = \omega_0 + \Delta\omega(\Delta\omega \ll \omega_0)$, the input impedance of the resonator

$$\begin{aligned} Z_{\text{in}} &= -jZ_{\text{msl}} \cot(\beta l) \\ &= -jZ_{\text{msl}} \cot\left(\frac{\pi}{2} + \frac{\pi\Delta\omega}{2\omega_0}\right) \\ &\approx jZ_{\text{msl}} \frac{\pi\Delta\omega}{2\omega_0} \end{aligned} \tag{2}$$

whereas its counterpart in the equivalent circuit Fig. 3(b) looking into the LC series resonator can be expressed by

$$Z_{\text{in}} = j\omega_0 L \left(\frac{\omega_0 + \Delta\omega}{\omega_0} - \frac{\omega_0}{\omega_0 + \Delta\omega}\right) \approx j\omega_0 L \cdot \frac{2\Delta\omega}{\omega_0}. \tag{3}$$

Comparing (3) with (2) leads to the inductance of the equivalent circuit

$$L = \frac{\pi Z_{\text{msl}}}{(4\omega_0)}. \tag{4}$$

Thus, (1) for the external Q reduces to

$$Q_e = {n_2}^2 \sqrt{\frac{L}{C}} \frac{1}{R} = \frac{{n_2}^2 \pi Z_{\text{msl}}}{4R}. \tag{5}$$

If the external Q can be measured from reflection coefficient S_{11}, then the coupling coefficient n_2 can be determined by (5).

By examining Fig. 3 and using the definition of an ideal transformer, the reflection coefficient looking at the input port of the microstrip line is given by

$$S_{11} = S'_{11} = \frac{Z_{\text{in}} - R'}{Z_{\text{in}} + R'}, \qquad \text{where } R' = \frac{R}{n^2}. \tag{6}$$

More specifically,

$$S_{11} = \frac{-jZ_{\text{msl}} \cot(\beta l) - \dfrac{\pi Z_{\text{msl}}}{4Q_e}}{-jZ_{\text{msl}} \cot(\beta l) + \dfrac{\pi Z_{\text{msl}}}{4Q_e}} = |S_{11}| e^{-2j\phi} \tag{7}$$

where $\phi = \tan^{-1}(\pi \tan(\beta l)/4Q_e)$.

It can be found that, at resonance, the group delay of the reflection coefficient is

$$\tau_{S_{11}}(\omega_0) = \frac{4Q_e}{\omega_0}. \tag{8}$$

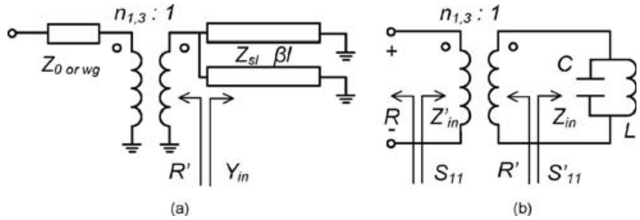

Fig. 4. (a) Coupling circuit between a transmission line (microstrip or waveguide) and a pair of short-circuited shunt $\lambda/4$ resonators by an ideal transformer. (b) Corresponding lumped-element circuit model.

The above relation is not new and is valid for any single resonator circuit [14]. Once Q_e is obtained from (8), the coupling coefficient n_2 can be determined by (5).

B. *Coupling Coefficients to U-Shaped Slotline Resonator*

At resonant frequency, the open-circuited quarter-wavelength resonator short circuits transformer 2. Therefore, the coupling n_1 and n_2 to a U-shaped slotline resonator become isolated. Thus, the coupling circuit between the transmission line, which could be either a microstrip line or a waveguide, and the half-wavelength slotline resonator can be represented by an ideal transformer, as shown in Fig. 4(a), where input admittance is given by

$$Y_{\text{in}} = -\frac{j2\cot(\beta l)}{Z_{sl}}. \tag{9}$$

Since a short-circuited quarter-wavelength transmission line can be approximated by a shunt LC tank, the physical circuit of a transmission line that is coupled to the half-wavelength U-shaped slotline resonator, as shown in Fig. 4(a), can be represented by the lumped element circuit of Fig. 4(b).

By a similar procedure as that for finding coupling coefficient n_2, it can be obtained that

$$Q_e = \omega_0 CR' = \frac{\pi R'}{2Z_{sl}} = \frac{\pi R}{2n_{1,3}^2 Z_{sl}} \tag{10}$$

and that the group delay of the reflection coefficient is related to the external Q by (8). Note that the notation $n_{1,3}$ refers to the coupling coefficient n_1 or n_3.

IV. Design of Physical Dimensions

The detailed guideline for designing physical dimensions of the proposed transition is illustrated by a design example of a broadband transition between a microstrip line and a ridge waveguide. Fig. 5(a) shows a centered longitudinally cross-sectional view of the microstrip-to-ridge waveguide transition. Fig. 5(b)–(d) are plan views of the reference planes A–A', B–B', and C–C', respectively. The related dimensional variables of the transition are also given in Fig. 5.

With the aid of the equivalent-circuit model discussed in Section III, an optimal circuit model for a given frequency band of interest, the characteristic impedances of the microstrip line and the ridged-waveguide dimension can be obtained by adjusting or optimizing the parameters in the circuit model shown in Fig. 2 using a circuit simulator such as Agilent ADS software. Due to the simplicity of the equivalent-circuit model,

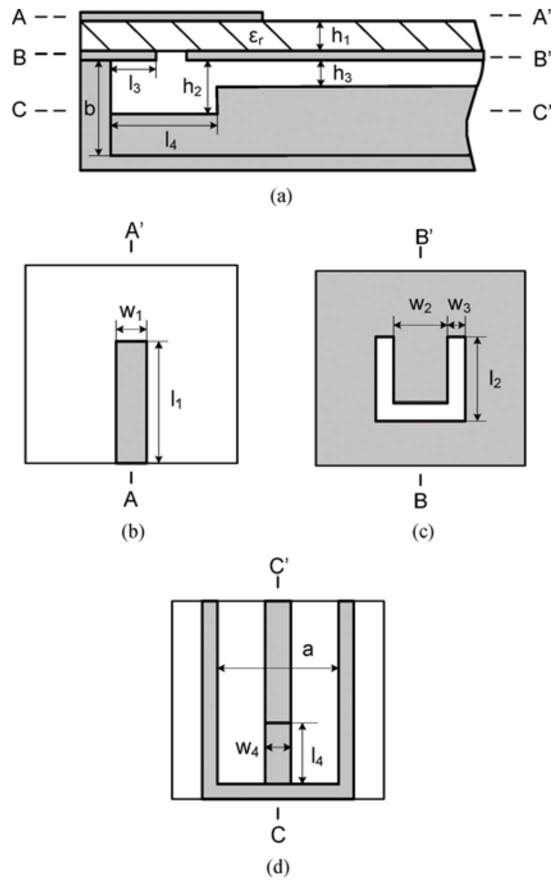

Fig. 5. Dimensions of the microstrip-to-ridged-waveguide transition.

it takes nearly no time to optimize the circuit model that operates in the desired frequency bandwidth. The optimized circuit model should provide all the realizable coupling coefficients and serve as the coarse model in a space-mapping optimization process, whereas the Ansoft HFSS EM simulation software is used as the fine model for designing the physical structure [15].

It is known that changing the width of the slotline not only changes the characteristic impedance, but also affects its couplings to the input/output transmission lines. With a given slotline width, the total length of the U-shaped slotline is designed to be approximately half guided wavelength according to the designed circuit model.

Fig. 6(a)–(c) shows the physical models for the determining coupling coefficients n_1, n_2, and n_3 in the equivalent circuit of Fig. 2, respectively.

Since the open-circuited quarter-wavelength resonator is nearly short circuited at the point extended to the edge of the slotline, in the physical model for calculating n_1, the microstrip line crossing-over the U slotline will be short circuited to ground, as shown in Fig. 6(a). It can be seen from Fig. 2 that when calculating coupling n_2, the U slotline resonator must be detuned so that no energy is divided. In addition, the dominant factor for determining coupling n_2 is the discontinuity of the section of slotline that divides the microstrip line and the quarter-wavelength open-circuited resonator. Therefore, for calculating coupling n_2, one only needs to consider a simplified physical model that consists of a short section of the slotline,

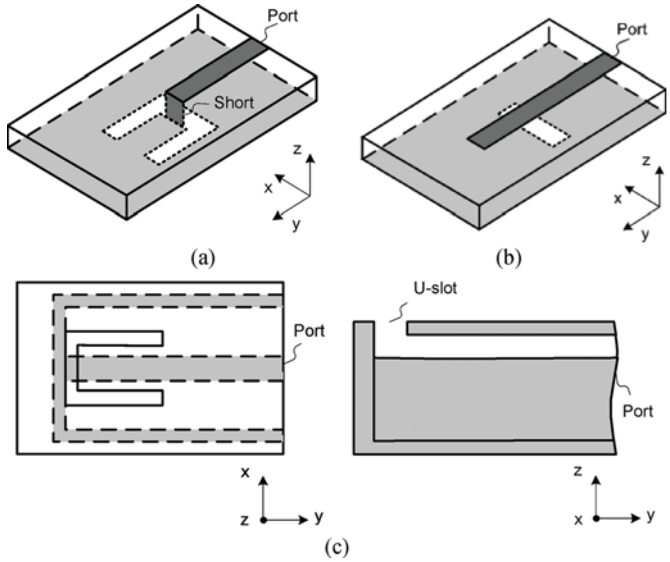

Fig. 6. Physical models for calculating the coupling coefficients.

as shown in Fig. 6(b). By the same token as that for calculating n_1, the coupling coefficient n_3 can be calculated with the simplified model given by Fig. 6(c) in which a true short-circuited node is realized by the waveguide end wall naturally. In other words, the waveguide end wall should not be placed too far from the middle section of the slotline resonator. In the design procedure, the required couplings can be determined one by one independently by using the group-delay information of each corresponding simplified physical model at the center frequency and with appropriate reference planes.

Having had an optimized circuit model, the initial physical dimensions of a transition can be obtained by the above-mentioned process. The final dimensions will be determined by a few steps of tuning using the concept of space-mapping optimization technique, which are: 1) EM simulation response of an nonoptimized transition (fine model) is curve fitted by the response of corresponding circuit model described by Fig. 2 (coarse model); 2) the extracted circuit model is compared to the optimized circuit model (golden template) for obtaining the error vector; and 3) a new EM simulation will be conducted using the updated fine model according to the error vector. The process will be repeated for a few iterations. Once the extracted circuit model is close enough to the golden template, an optimized transition design is achieved.

V. Design Examples

In this section, the claimed features will be demonstrated by two design examples by following the design procedure outlined in Section IV.

A. Example 1

In this design example, a surface mountable broadband ridged-waveguide bandpass filter with microstrip line as filter interface is investigated. The detailed design procedure of a microstrip-to-ridge-waveguide transition is given here, where a 50-Ω microstrip line printed on the substrate is used for both microstrip line and the quarter-wavelength resonator. Rogers Duroid 5870 substrate with dielectric constant of 2.33 and loss tangent of 0.0012 is used. The U-shaped slotline and the ridged waveguide are with the characteristic impedance of 160 and 88 Ω, which were calculated by closed-form formulas given in [16] and [17], respectively. With the impedances are chosen, the other circuit parameters in the circuit model shown in Fig. 2 can be easily optimized to achieve maximum bandwidth and are given in Table I. Having had required coupling coefficients, the design equations and the segregated physical coupling models described in Sections III and IV can be applied directly to obtain the initial dimensions. The obtained initial, as well optimized, final physical dimensions are summarized in Table II. Fig. 7 shows the S-parameters of the initial EM model, the optimal circuit model, and the final EM designed model. The EM simulation is done by commercial Ansoft HFSS software. To verify the proposed circuit model, the final EM designed responses are curve fitted for extracting its corresponding circuit parameters according to the circuit model shown in Fig. 2. The extracted circuit parameters are also listed in Table I for comparative purposes. A slight discrepancy in the resonance frequencies of the quarter-wavelength resonators is caused by the parasitic effects of the open end and the bends of the U-shaped slotline resonator. The excellent agreement of the designed and the extracted coupling coefficients demonstrates that the proposed circuit model is fully competent for a practical engineering design.

The EM simulated results in Fig. 7 show that more than 55% bandwidth for the return loss of better than 15 dB across the whole frequency band can be achieved. To show the broadband feature of a standalone transition, a back-to-back test module

TABLE I
Comparison of the Circuit Model Parameters

Circuit Model Parameters	Optimal Designed	Extracted
n_1	0.876	0.884
n_2	1.136	1.139
n_3	1.321	1.372
f_0 of open-circuited λ/4 resonator	7.75 GHz	7.56 GHz
f_0 of parallel short-circuited λ/4 resonator	5.24 GHz	5.7 GHz

TABLE II
Dimensions of the Transition in Millimeters

Variables	Initial	Final	Variables	Initial	Final
a	13.00	13.00	l_1	8.42	9.35
b	6.00	6.00	l_2	12.25	11.50
w_1	4.40	4.40	l_3	0.00	0.80
w_2	3.00	5.50	l_4	-	6.50
w_3	1.50	1.50	h_1	1.58	1.58
w_4	2.40	2.40	h_2	0.60	2.40
			h_3	0.60	0.60

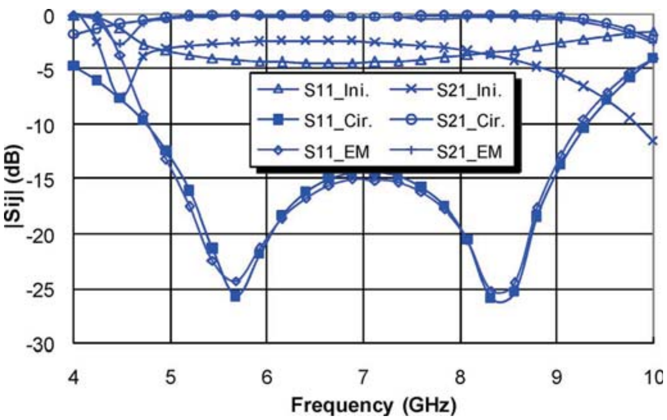

Fig. 7. Simulated results of the equivalent-circuit model and EM model of the microstrip-to-ridge-waveguide transition.

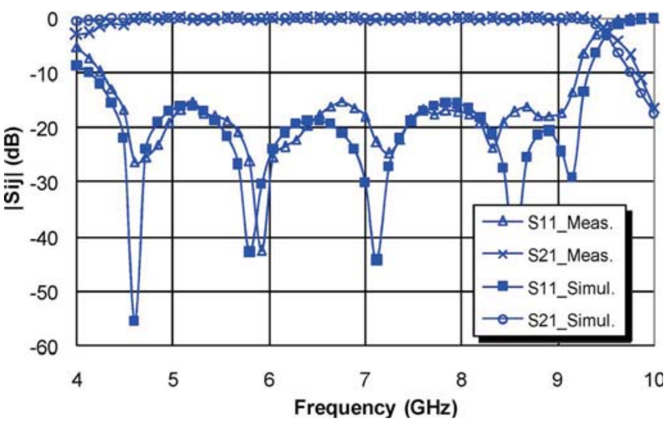

Fig. 8. Measured and simulated S-parameters of the back-to-back microstrip-to-ridge-waveguide transition module.

was designed, manufactured, and tested. The measured and EM simulated S-parameters of the test module are superimposed in Fig. 8. The measured in band insertion loss of the back-to-back module is better than 0.5 dB from 4.6 to 9.1 GHz with a return loss better than 15 dB. It can be derived that the measured insertion loss of a single transition will be better than 0.2 dB from 4.6 to 9.1 GHz. Very good agreement between the simulated and measured firmly proves the concept of the proposed compact broadband transition and the circuit model.

With the designed transition, a broadband ridged-waveguide bandpass filter with microstrip interfaces is designed using ten ridge post resonators and 11 evanescent mode rectangular waveguide as coupling sections. The heights of each ridge post resonator are set to be the same and the structure of the filter is symmetric both in the transversal and the longitudinal directions. The cross-sectional views of the filter is given in Fig. 9, in which the microstrip line that is printed on a Duroid 5870 substrate and the transition are not shown in this figure.

An in-house full-wave EM simulation based on mode-matching theory is applied for designing the ridged-waveguide filter with ridged-waveguide interfaces. Having merged the transition design with the filter design that is conducted separately into one entity, the final structure needs slight tuning at the input/output sections to accommodate the higher order mode effect. The designed filter dimensions are given in Table III.

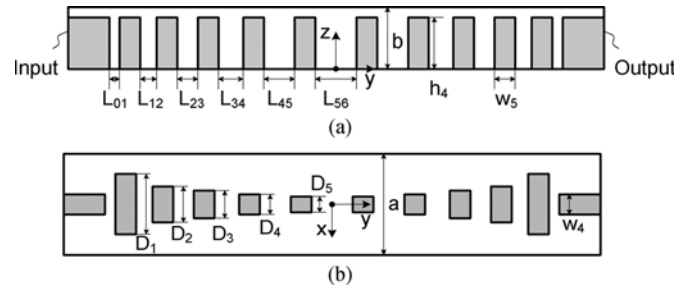

Fig. 9. Sectional view of the ridged-waveguide filter. (a) Side view. (b) Top view.

TABLE III
DIMENSIONS OF THE FILTER IN MILLIMETERS

a	13.00	l_3	3.60	D_5	2.02
b	6.00	l_4	6.70	L_{01}	1.31
w_1	4.40	h_1	1.58	L_{12}	4.52
w_2	4.80	h_2	3.60	L_{23}	5.89
w_3	1.10	h_3	0.60	L_{34}	6.26
w_4	2.40	D_1	7.42	L_{45}	6.39
w_5	2.40	D_2	2.61	L_{56}	6.42
l_1	14.80	D_3	2.12		
l_2	11.00	D_4	2.04		

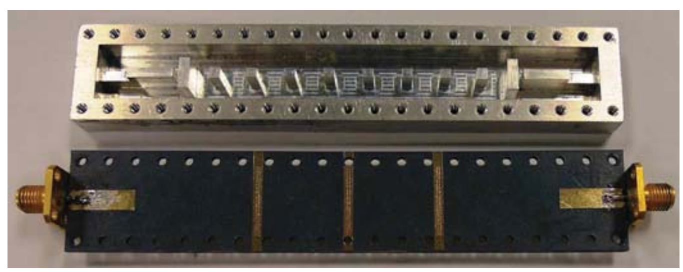

Fig. 10. Photograph of the ridged-waveguide broadband bandpass filter with the microstrip-to-waveguide transition.

The filter is fabricated with an ordinary milling machine and the photograph of the filter is shown in Fig. 10. The measured and EM S-parameters are superimposed in Fig. 11, showing a good broadband characteristic of nearly 2-GHz bandwidth with the return loss next to 20 dB.

B. Example 2

Laminated waveguides not only provides a low-loss attribute similar to traditional waveguide, but they also provides manufacturability in a planar multilayered fashion. In this example, an integrated LTCC laminated waveguide cavity filter with the interface of a microstrip line is designed, fabricated, and tested. The substrate tape used is Dupont 951 with the dielectric constant of 7.6 and loss tangent of 0.006. The thickness of each green tape layer is 0.095 mm. The laminated waveguide and microstrip line substrate occupies eight and four layers, respectively. A microstrip-to-laminated-waveguide transition for a given desired frequency band is designed using the design

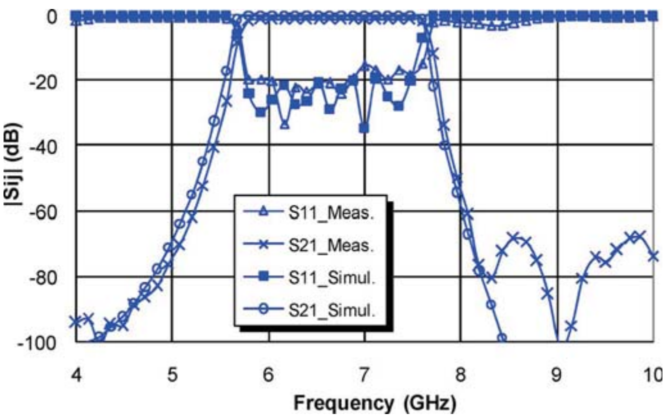

Fig. 11. Measured and simulated S-parameters of the broadband ridged-waveguide filter with microstrip interfaces.

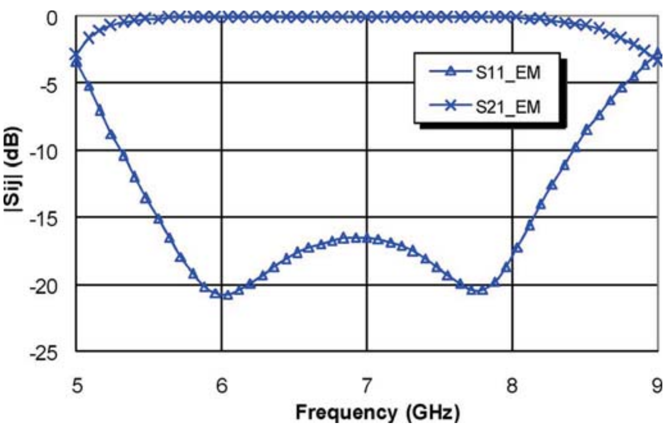

Fig. 12. Simulated performance of a single microstrip-to-laminated-waveguide transition.

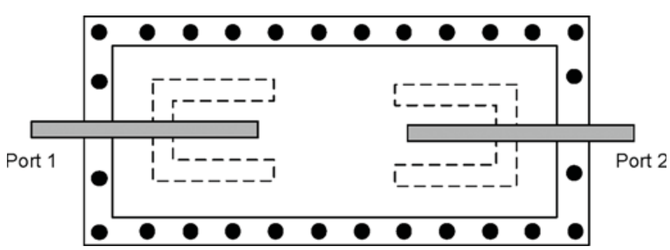

Fig. 13. Top view of the back-to-back transition between a microstrip and an LTCC laminated waveguide.

procedure similar to that in design example 1. The designed performance of a single transition is shown in Fig. 12. The back-to-back transition module, as illustrated in Fig. 13, is also prototyped and tested, whose measured and simulated results are shown in Fig. 14. The measured magnitudes of S-parameters indicate that in-band insertion loss is better than 0.76 dB from 5.8 to 8.2 GHz with a return loss better than 15 dB. Thus, the measured insertion loss of a single transition will be better than 0.38 dB from 5.8 to 8.2 GHz.

The structure and dimensions of the laminated waveguide filter are shown in Fig. 15, which consists of four inline laminated waveguide cavity resonators. The dominant TE_{101} mode is excited in each half-wavelength resonator. The inter-resonator couplings are realized by inductive irises. Using an HFSS solver, the optimum filter parameters can be obtained after a few steps of fine tuning and are provided in Table IV. The photograph of the laminated waveguide filter with interfaces to microstrip is illustrated in Fig. 16. The measured and simulated results presented in Fig. 17 are in good agreement. It is seen that the filter is with a bandwidth of 0.7 GHz at center frequency of 7.1 GHz and is with the return loss better than 20 dB. The insertion of the filter module near center frequency

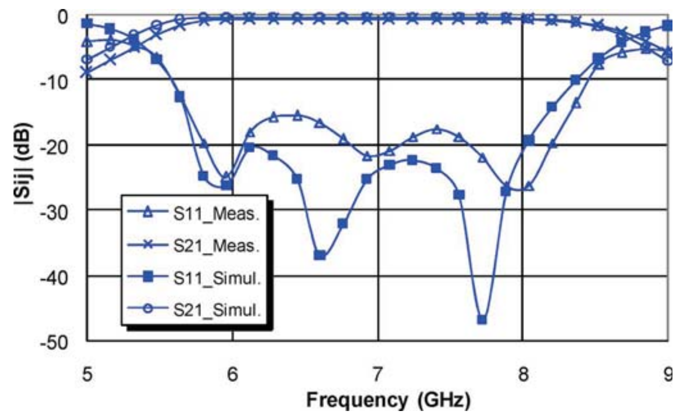

Fig. 14. Measured and simulated S-parameters of the back-to-back microstrip to LTCC laminated waveguide transition module.

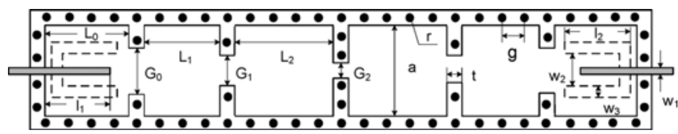

Fig. 15. Structure and dimensions of the LTCC laminated waveguide filter.

TABLE IV
DIMENSIONS (UNIT: MILLIMETERS) OF THE LAMINATED WAVEGUIDE FILTER

a	10.40	l_2	5.15	G_1	4.36
r	0.08	L_0	11.90	G_2	4.00
g	0.65	L_1	8.25	w_1	0.35
t	0.24	L_2	9.25	w_2	1.10
l_1	7.00	G_0	6.15	w_3	1.25

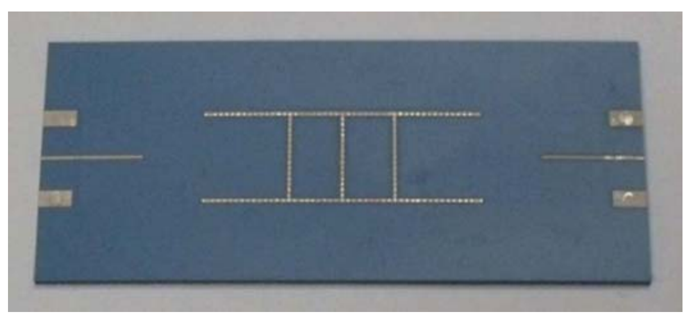

Fig. 16. Photograph of the LTCC laminated waveguide filter.

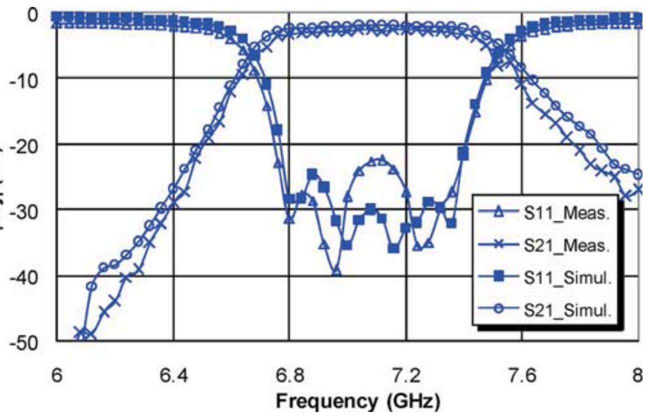

Fig. 17. Measured and simulated S-parameters of the LTCC laminated waveguide filter with microstrip interfaces.

is about 2.5 dB. It is worth mentioning that the laminated LTCC cavity filter module is designed to be surface mountable. Its insertion loss can be improved by increasing the thickness of the cavities.

VI. Conclusion

This paper has presented a novel broadband microstrip-to-waveguide transition. A more than 55% bandwidth for the return loss better than 15 dB has been demonstrated in C-band. In addition to the broadband feature, it is compact in size, convenient for mass production, and highly compatible with planar circuits. A physics-based equivalent-circuit model and an initial design procedure are also developed. The circuit model clearly reveals the working mechanism of the transition and can be used as a very pertinent coarse model in using the space-mapping optimization technique. The developed formulas and the simplified models for calculating coupling coefficients can provide a very good starting point. Two typical uses of the transition in C-band applications are given: one for a broadband ridged-waveguide bandpass filter and one for an integrated LTCC laminated waveguide bandpass filter. Both theoretic and measured results have demonstrated its versatile applications and its excellent performance in terms of broad bandwidth and low insertion loss.

References

[1] J. C. Hoover and R. E. Tokheim, "Microstrip transmission-line transitions to dielectric-filled waveguide," *IEEE Trans. Microw. Theory Tech.*, vol. MTT-15, no. 4, pp. 273–274, Apr. 1967.

[2] F. J. Villegas, D. I. Stones, and H. A. Hung, "A novel waveguide-to-microstrip transition for millimeter-wave module applications," *IEEE Trans. Microw. Theory Tech.*, vol. 47, no. 1, pp. 48–55, Jan. 1999.

[3] N. Kaneda, Y. Qian, and T. Itoh, "A broadband microstrip-to-waveguide transition using quasi-Yagi antenna," *IEEE Trans. Microw. Theory Tech.*, vol. 47, no. 12, pp. 2562–2567, Dec. 1999.

[4] J. H. C. Van Heuven, "A new integrated waveguide-microstrip transition," *IEEE Trans. Microw. Theory Tech.*, vol. MTT-24, no. 3, pp. 144–147, Mar. 1976.

[5] H.-S. Oh and K.-W. Yeom, "A full Ku-band reduced-height waveguide-to- microstrip transition with a short transition length," *IEEE Trans. Microw. Theory Tech.*, vol. 58, no. 9, pp. 2456–2462, Sep. 2010.

[6] Y. Lou, C. H. Chan, and Q. Xue, "An in-line waveguide-to-microstrip transition using radial-shaped probe," *IEEE Microw. Wireless Compon. Lett.*, vol. 18, no. 5, pp. 311–313, May 2008.

[7] H. W. Yao, A. Abdelmonem, J. F. Liang, and K. A. Zaki, "Analysis and design of microstrip-to-waveguide transitions," *IEEE Trans. Microw. Theory Tech.*, vol. 42, no. 12, pp. 2371–2380, Dec. 1994.

[8] Y. Ding and K. Wu, "Substrate integrated waveguide-to-microstrip transition in multilayer substrate," *IEEE Trans. Microw. Theory Tech.*, vol. 55, no. 12, pp. 2839–2844, Dec. 2007.

[9] D. Deslandes and K. Wu, "Integrated microstrip and rectangular waveguide in planar form," *IEEE Microw. Wireless Compon. Lett.*, vol. 11, no. 2, pp. 68–69, Feb. 2001.

[10] B. N. Das, K. V. S. V. R. Prasad, and K. V. S. Rao, "Excitation of waveguide by stripline- and microstrip-line-fed slots," *IEEE Trans. Microw. Theory Tech.*, vol. MTT-34, no. 3, pp. 321–327, Mar. 1986.

[11] W. Grapher, B. Hudler, and W. Menzel, "Microstrip to waveguide transition compatible with mm-wave integrated circuits," *IEEE Trans. Microw. Theory Tech.*, vol. 42, no. 9, pp. 1842–1843, Sep. 1994.

[12] L. Hyvonen and A. Hujanen, "A compact MMIC-compatible microstrip to waveguide transition," in *IEEE MTT-S Int. Microw. Symp. Dig.*, San Francisco, CA, 1996, vol. 2, pp. 875–878.

[13] L. T. Hildebrand and J. Joubert, "Full-wave analysis of a new microstrip-to-waveguide interconnect configuration," *IEEE Trans. Microw. Theory Tech.*, vol. 48, no. 1, pp. 1–7, Jan. 2000.

[14] J. S. Hong and M. J. Lancaster, *Microstrip Filters for RF/Microwave Applications*. New York: Wiley, 2001, sec. 8.4.

[15] J. W. Bandler, R. M. Biernacki, S. H. Chen, R. H. Hemmers, and K. Madsen, "Electromagnetic optimization exploiting aggressive space mapping," *IEEE Trans. Microw. Theory Tech.*, vol. 43, no. 12, pp. 2874–2882, Dec. 1995.

[16] R. Garg, P. Bhartia, I. Bahl, and A. Ittipaboon, *Microstrip Antenna Design Handbook*. Norwood, MA: Artech House, 2001, pp. 786–789.

[17] W. J. R. Hoefer and M. N. Burton, "Closed-form expressions for the parameters of finned and ridged waveguides," *IEEE Trans. Microw. Theory Tech.*, vol. MTT-30, no. 12, pp. 2190–2194, Dec. 1982.

Xiaobo Huang was born in Jiangsu, China, in 1983. He received the B.Eng. and M.Eng. degrees in electronic and optical engineering from the Nanjing University of Science and Technology, Nanjing, China, in 2005 and 2007, respectively, and the Ph.D. degree in electronic engineering from The Chinese University of Hong Kong, Shatin, Hong Kong, in 2011.

Since 2011, he has been a Research Engineer with the China Research and Development Center, Comba Telecommunication Systems, Guangzhou, China, where he is involved with LTE smart antennas. His current research interests include passive microwave and millimeter-wave circuits, antennas and filters for communication systems, and LTCC-based modules for wireless communications.

Ke-Li Wu (M'90–SM'96–F'11) received the B.S. and M.Eng. degrees from the Nanjing University of Science and Technology, Nanjing, China, in 1982 and 1985, respectively, and the Ph.D. degree from Laval University, Quebec, QC, Canada, in 1989.

From 1989 to 1993, he was with the Communications Research Laboratory, McMaster University, as a Research Engineer and a Group Manager. In March 1993, he joined the Corporate Research and Development Division, COM DEV International, where he was a Principal Member of Technical Staff. Since October 1999, he has been with The Chinese University of Hong Kong, Shatin, Hong Kong, where he is a Professor and the Director of the Radiofrequency Radiation Research Laboratory (R3L). He has authored or coauthored numerous publications in the areas of EM modeling and microwave and antenna engineering. His current research interests include partial element equivalent circuit (PEEC) and derived physically expressive circuit (DPEC) EM modeling of high-speed circuits, RF and microwave passive circuits and systems, synthesis theory and practices of microwave filters, antennas for wireless terminals, LTCC-based multichip modules (MCMs), and RF identification (RFID) technologies.

Dr. Wu is a member of the IEEE MTT-8 Subcommittee (Filters and Passive Components) and is a Technical Program Committee (TPC) member for many international conferences including the IEEE Microwave Theory and Techniques Society (IEEE MTT-S) InternationalMicrowave Symposium (IMS). He was an associate editor for the IEEE Transactions on Microwave Theory and Techniques (2006–2009). He was the recipient of the 1998 COM DEV Achievement Award for the development of exact EM design software of microwave filters and multiplexers and the 2008 Asia–Pacific Microwave Conference Prize.